

See discussions, stats, and author profiles for this publication at: <https://www.researchgate.net/publication/318475515>

# Analytical Solutions of Three-Dimensional Contaminant Transport Models with Exponential Source Decay

Article in *Ground Water* · July 2017

DOI: 10.1111/gwat.12564

---

CITATIONS

21

---

READS

725

## 4 authors:



**Ombretta Paladino**

Università degli Studi di Genova

101 PUBLICATIONS 687 CITATIONS

SEE PROFILE



**Arianna Moranda**

Università degli Studi di Genova

11 PUBLICATIONS 73 CITATIONS

SEE PROFILE



**Marco Massabó**

CIMA Research Foundation

52 PUBLICATIONS 357 CITATIONS

SEE PROFILE



**Gary Robbins**

University of Connecticut

85 PUBLICATIONS 1,399 CITATIONS

SEE PROFILE

Some of the authors of this publication are also working on these related projects:



Fate & transport of pollutants in groundwater [View project](#)



Environmental & Human Health Risk Assessment of Chemicals [View project](#)

Research paper

## **Analytical solutions and approximation errors of 3D contaminant transport models with exponential source decay**

### **Ombretta Paladino**

Corresponding author: Dipartimento di Ingegneria Civile, Chimica e Ambientale, Università degli Studi di Genova - Via Opera Pia 15, 16145 Genova; paladino@unige.it

### **Arianna Moranda**

Dipartimento di Ingegneria Meccanica, Energetica, gestionale e dei trasporti, Università degli Studi di Genova - Piazzale Kennedy, 16100 Genova.

### **Marco Massabò**

CIMA Research Foundation - Via Magliotto 2, 17100 Savona.

### **Gary A. Robbins**

Department of Natural Resources and the Environment, University of Connecticut, 1376 Storrs Road, Storrs, Connecticut 06269, USA.

**Conflict of interest:** None

**Keywords:** groundwater modeling, 3D analytical solutions, source decay

- 1 **Article Impact Statement:** A 3D closed form solution of advection-dispersion-equation for
- 2 reacting solute with source decay, suitable for Tier I risk analysis.

### 3 **Abstract**

4 Despite the availability of numerical models, interest in analytical solutions of multi-dimensional  
5 advection-dispersion systems remains high. Such models are commonly used for performing  
6 Tier I risk analysis and are embedded in many regulatory frameworks dealing with ground water  
7 contamination. In this work we develop a closed form solution of the 3D advection-dispersion-  
8 equation (ADE) with exponential source decay, first order reaction and retardation, and present  
9 an approach based on some ease of use diagrams to compare it with the integral open form  
10 solution and with earlier versions of the closed form solution. The comparison approach focuses  
11 on the relative differences associated with source decay and the effect of simulation time. The  
12 analysis of concentration contours, longitudinal sections and transverse sections confirms that the  
13 closed form solutions studied can be used with acceptable approximation in the central area of a  
14 plume bound transversely within the source width, both behind and beyond the advective front  
15 and for concentration values up to two orders of magnitude less than the initial source  
16 concentration. Since the proposed closed form model can be evaluated without nested numerical  
17 computations and with simple mathematical functions, it can be very useful in risk assessment  
18 procedures.

19

### 20 **Introduction**

21 Analytical and semi-analytical solutions are efficient tools widely used for modeling fate  
22 and transport of contaminants in groundwater. These solutions are useful for testing complex  
23 numerical transport models under particular simplified subsurface and boundary conditions and  
24 for performing risk analysis of polluted sites resulting from accidental spills and waste disposal

25 activities. Modern numerical transport models are capable of handling multi-contaminant  
26 systems with complex reaction chains in non-homogeneous and anisotropic media, under a  
27 multitude of initial and boundary conditions. Unfortunately, complex numerical models require  
28 defining parameters which are often not well known, leading to model outputs that are highly  
29 uncertain. This uncertainty in some cases could diminish the advantages of adopting a more  
30 detailed approach. During the past decades a great number of analytical solutions of the  
31 advection-dispersion equation for both conservative and reacting solutes have been developed.  
32 These solutions have been developed to provide physical insights into transport problems and  
33 they are also preferred by governments and some companies to perform Tier I risk assessments  
34 because of their ease of use and low costs for implementation (Ford et al, 2007).

35 Sagar (1982), Wexler (1992), Batu (1993) proposed exact 3D analytical solutions in  
36 integral open form. Batu (1996, 2006) proposed a generalized open form 3D analytical solution  
37 containing series; Leij et al. (2000) provided a useful collection of 3D solutions by applying  
38 Green's Function Method (GFM). Park and Zhan (2001) and Wang and Wu (2009) provided  
39 one-, two- and three dimensional analytical solutions in both closed form and integral open form  
40 in an aquifer of finite thickness by using GFM. Wang et al. (2011) proposed a stepwise  
41 superposition approach for the analytical solution in infinite and finite domains expressed as  
42 sums rather than integrals.

43 A major limitation in all the aforementioned multi-dimensional analytical solutions in  
44 finite-infinite domains and under first or third type boundary conditions include integrals in their  
45 expression or infinite series, which need to be solved numerically. The numerical solutions can  
46 introduce approximation errors, can be computationally demanding and may explain why models  
47 using the same input parameters can generate very different results.

48

49 Domenico and Robbins (1985), Domenico (1987), Martin-Hayden and Robbins (1997)  
50 proposed some 3D approximated analytical solutions in closed form. The key advantage of the  
51 Domenico and Robbins (1985) approach and its derived extensions included in US EPA tools as  
52 BIOSCREEN (1996), BIOCHLOR (Aziz et al., 2000), currently used in risk assessment  
53 procedures, is that it provides a closed form solution that can be evaluated with much less  
54 significant numerical computations since it contains only complementary error functions. The  
55 latest version of the Domenico-Robbins-based solutions is valid for linear sorption, pollutant first  
56 order decay and a variety of plane and linear source boundary conditions. These analytical  
57 solutions, identified by the authors as based on the "extended-pulse-approximation", have  
58 received much attention in the literature, given their adoption by regulatory agencies.

59 By recalling the principal steps followed by Domenico and Robbins (1985), it can be  
60 noticed that they propose a closed form 3D solution by multiplying the 1D solution in the flow  
61 direction with the two transverse spreading solutions, in which time  $t$  is replaced by an averaged  
62 time taken as  $x/v$ , where  $x$  is the coordinate in the flow direction and  $v$  is the average pore scale  
63 velocity. Wexler (1992) provided an exact analytical solution of the equation proposed in  
64 Domenico (1987), this solution was already contained in the work by Sagar (1982). Srinivasan et  
65 al. (2007) performed a limiting analysis of the approximated Domenico (1987) solution and  
66 proved that it relaxes to the Wexler (1992) analytical solution for axial dispersivity tending to  
67 zero. Srinivasan et al. (2007) concluded that the Domenico and Robbins (1985) approach forces  
68 a quasi-steady state condition in transverse direction at all times, and for this reason it introduces  
69 significant errors for longitudinal-dominated problems. They performed some comparison by  
70 varying dispersivities and space velocity by an order of magnitude, showing the possibility of

71 high errors in the centerline. Also West et al. (2007) performed comparisons with the Domenico  
72 and Robbins-modified solutions, along the centerline, by varying the source dimension and  
73 dispersion coefficients. Their results gave errors of about 40-80% at small simulation times.  
74 Guyonnet and Neville (2004) performed a comparison method using non-standard dimensionless  
75 groups and on the axial Peclet number, finding errors in the transverse direction greater than in  
76 the axial one.

77 In this work we present a new closed form solution of the 3D problem with first order  
78 reaction and retardation but unlike past solutions allows for exponential source decay. The  
79 model being suitable for treating continuous source dissipation with time owing to dilution by  
80 precipitation or source removal or remediation. We also suggest a novel approach to compare  
81 models using some ease of use diagrams that include all the previous analytical solutions. The  
82 comparison approach can be extended to other solutions in finite domain and different shaped  
83 sources. The particular solution here analyzed in detail refers to a plane source with first type  
84 boundary condition, semi-finite domain in x direction and infinite domain in y and z directions.  
85 Concentration at the source is defined as a decaying exponential function of time.

## 86 **Model derivation**

87 The governing equation for the three-dimensional advection-dispersion of a solute subject  
88 to a first order decay (also valid for a pseudo-first order reaction in homogeneous phase where  
89 the contaminant is the controlling reactant, i.e. other reactants are in excess) and linear sorption,  
90 instantaneous and reversible, can be written as:

$$91 \quad R \frac{\partial c}{\partial t} = -v \frac{\partial c}{\partial x} + D_x \frac{\partial^2 c}{\partial x^2} + D_y \frac{\partial^2 c}{\partial y^2} + D_z \frac{\partial^2 c}{\partial z^2} - \lambda c \quad (1)$$

92 where  $c(x, y, z, t)$  is the solute concentration  $[ML^{-3}]$ ,  $x$  is the longitudinal coordinate,  $y$  and  $z$  are  
93 the horizontal transverse and the vertical coordinates, respectively,  $v$  is the average pore scale  
94 velocity of the fluid  $[LT^{-1}]$ , taken unidirectional along  $x$ ,  $D_x$  is the longitudinal dispersion  
95 coefficient  $[L^2T^{-1}]$ ,  $D_y$  and  $D_z$  are the horizontal transverse and the vertical transverse dispersion  
96 coefficients  $[L^2T^{-1}]$ , respectively,  $t$  is time  $[T]$ ,  $\lambda$  is the first order decay constant  $[T^{-1}]$ , and  $R$  is  
97 the retardation factor  $[-]$ .

98 The retardation factor can be eliminated from the term on the left by replacing  $D_x$ ,  $D_y$ ,  $D_z$   
99 with  $D_x/R$ ,  $D_y/R$ ,  $D_z/R$ ;  $v$  with  $v/R$  and,  $\lambda$  with  $\lambda/R$ .

100 Eqn. (1) can be written as a linear operator on concentration:

$$101 \quad L(C(x, y, z, t)) = 0 \quad (2)$$

102 By applying the GFM it is possible to obtain different solutions depending on different  
103 boundary and initial conditions (Greenberg 1971, Roach 1982). It is possible to use GFM if the  
104 following conditions occur:

- 105 1) homogeneous and anisotropic porous medium;
- 106 2) constant velocity in  $x$  direction;
- 107 3) horizontally infinite or semi-finite domains; vertically semi-finite or finite domains;
- 108 4) initial condition set as  $c(x, y, z, 0) = 0$
- 109 5) point, linear, plane, volumetric source (regular or irregular).

110 The source of contamination can be usually placed as:

- 111 i. a source generation term  $r [ML^{-3}T^{-1}]$  inside the domain (GFM general approach) and in  
112 this case an infinite domain in  $x$  and  $y$  is usually considered;

113 ii. a boundary condition of the first type and expressed as concentration, or a boundary  
 114 condition of the third type and expressed as a mixed flux/concentration in a semi-finite  
 115 domain.

116 If we consider case i), i.e. the source term inside the domain, usually we put:

$$117 \quad c(\infty, y, z, t) = 0 \quad (3)$$

$$118 \quad c(x, \pm\infty, z, t) = 0 \quad (4)$$

$$119 \quad c(x, y, \pm\infty, t) = 0 \quad \left( \text{or } \frac{\partial c}{\partial z} = 0 \text{ in } z \text{ direction, where the domain is finite} \right) \quad (5)$$

120

121 The specific source generation term (source strength) can be defined as:

$$122 \quad r = \begin{cases} r_0 f(t) & 0 < x < x_0; y_0 < y < y_1; z_0 < z < z_1 \\ 0 & \end{cases} \quad (6)$$

123 where  $r$  is a function of  $x, y, z$  and can be a linear or non-linear function of  $t$ ;  $r_0$  [ $\text{ML}^{-3}\text{T}^{-1}$ ] is the  
 124 initial volumetric mass released by the source per unit of time,  $f(t)$  is a dimensionless known  
 125 function. The specific source generation term exists only in the space occupied by the source,  
 126 otherwise is zero. The specific source generation term cannot depend on  $C$ .

127 Since eqn. (1) is linear, the superposition principle allows us to write each appropriate Green's  
 128 function as the sum of a fundamental solution and a causal solution. The fundamental (or  
 129 source) solution is found by solving eqn. (1) under homogeneous boundary conditions at infinity  
 130 and with an added generation term  $r$ , discontinuous inside the domain and defined by:

$$131 \quad r = r_0 \delta(x - x_0) \delta(y - y_0) \delta(z - z_0) \delta(t - t_0) \quad (7)$$

132

133 The causal (or forced) solution is given by solving eqn. (1) under inhomogeneous  
 134 boundary conditions. Subsequently, it is possible to find the solution for distributed and/or  
 135 continuous generation terms as the superposition of the solutions obtained by describing the



136 generation terms as an infinite number of pulse functions. In summary, by knowing the solution  
 137 for the instantaneous point source (solved for infinite, semi-finite or finite domains), we can  
 138 extend it to a more complex source knowing that:

- 139 A. The 3D solution for a point instantaneous source is the product of the 3 directional  
 140 solutions;
- 141 B. The 3D solution for a finite instantaneous source can be obtained by integration of the 3D  
 142 point source solution into the source domain;
- 143 C. The 3D solution for a continuous (point or not-point) source can be obtained by  
 144 integration of the 3D source solution in time.

145 In case of finite boundaries it is possible to use the method of images (or reflection  
 146 method) to find the Green's function: starting from the free space solution we can add to it some  
 147 other solutions of eqn. (2) in order to get the required boundary condition. To do this, we can  
 148 suppose that there is an image of the source outside of the domain, with opposite sign and  
 149 exactly at the same distance away from the boundary as the source is (like a mirror). The goal is  
 150 to cancel the values of the free space solution that are on the boundaries. This method is used to  
 151 find solutions of the ADE for finite z domain (usually from 0 to L).

152 The analytical solution of eqn. (1) for the instantaneous point source centered in  
 153  $(x_0, y_0, z_0)$  at time  $t_0$  subject to (3), (4) and (5) is obtained by applying (A) to the well known  
 154 1D directional solutions:

$$\begin{aligned}
 c(x, y, z, t) = & \frac{M}{8\sqrt{\pi^3 D_x D_y D_z (t-t_0)^3}} \exp[-\lambda(t-t_0)] \exp\left\{-\frac{[(x-x_0)-v(t-t_0)]^2}{4D_x(t-t_0)}\right\} \\
 & \exp\left[-\frac{(y-y_0)^2}{4D_y(t-t_0)}\right] \exp\left[-\frac{(z-z_0)^2}{4D_z(t-t_0)}\right]
 \end{aligned} \tag{8}$$

156

157 where M is the total mass inserted by the instantaneous point source per unit time ( Baetsle,  
 158 1969). A class of solutions for the point source in different domains can be obtained by changing  
 159 equations (3), (4), (5) with different ones. Finally, it is possible to obtain analytical solutions for  
 160 complex sources in space and time by integrating the class of point solutions in space and time.

161 If we consider case ii), i.e. the source term is a boundary condition of the first type or  
 162 third type, the generation term  $r$  is zero and we have, respectively:

$$163 \quad c(0, y, z, t) = \begin{cases} c_0 f(t) & \text{or} \quad -D \frac{\partial c(0, t)}{\partial x} + vc(0, t) = vg(t) \\ 0 & \end{cases} \quad Y_1 < Y < Y_2; Z_1 < Z < Z_2 \quad (9)$$

$$164 \quad c(\infty, y, z, t) = 0 \quad \text{or} \quad \frac{\partial c(L_0, t)}{\partial x} = 0 \quad \text{or} \quad \frac{\partial c(\infty, t)}{\partial x} = 0 \quad (10)$$

$$165 \quad c(x, \pm\infty, z, t) = 0 \quad (11)$$

$$166 \quad c(x, y, \pm\infty, t) = 0 \quad (\text{or} \quad \frac{\partial c}{\partial z} = 0 \quad \text{in } z \text{ direction, where the domain is finite}) \quad (12)$$

167

168 where  $c_0$  [ML<sup>-3</sup>] is the initial source concentration,  $f(t)$  is a dimensionless time function,  $g(t)$  is a  
 169 time function and  $L_0$  [L] is the length of the finite x domain.

170 Sagar (1982) and Wexler (1992) derived the analytical solution of the 3D ADE for a  
 171 plane source described by a boundary condition of the first type at constant concentration  $c_0$ , and  
 172 the remaining boundary conditions expressed as concentration tending to zero at infinite domain  
 173 (terms on the left of eqns. (10), (11) and (12)).

174 The solution can be found by using traditional integration transform methods or GFM. The final  
 175 analytical solution is:

176

$$c(x, y, z, t) = \frac{C_0 x'}{8\sqrt{\pi D_x}} \int_0^t \exp\left[-\lambda\tau - \frac{(x'-v\tau)^2}{4D_x\tau}\right] \left[ \operatorname{erfc} \frac{y-y_2}{2\sqrt{D_y\tau}} - \operatorname{erfc} \frac{y-y_1}{2\sqrt{D_y\tau}} \right] \left[ \operatorname{erfc} \frac{z-z_2}{2\sqrt{D_z\tau}} - \operatorname{erfc} \frac{z-z_1}{2\sqrt{D_z\tau}} \right] \frac{1}{(\tau)^{3/2}} d\tau \quad (13)$$

178

179 where  $\tau = t - t_0$ ;  $x' = x - x_0$ .

180 It is important to remark that since Eqn. (13) satisfies the initial condition  $c(x, y, z, 0) = 0$ ,  
 181 the solution predicts a concentration equal to zero at  $x' = 0$  for every  $y$  and  $z$  and  $t = 0$ , as already  
 182 observed by Wang et al. (2011). So the solution is valid for all  $x' > 0$ .

183 Eqn.(13) is in open form and the integral in time has to be numerically evaluated. Wang  
 184 et al. (2011) introduced a stepwise superposition approach to handle eqn.(13) by discretizing the  
 185 time interval in  $N$  steps and by approximating the contribute of  $G_y \times G_z$  by its weighted average.

186 Martin-Hayden and Robbins (1997) proposed an analytical solution for a plane source in  
 187 closed form by adopting the approximation of Domenico (1987), this solution is referred by  
 188 Srinivasan et al. (2007) as the “modified-Domenico” solution. This analytical solution takes into  
 189 account the first order decay and is contained in BIOCHLOR (Aziz et al., 2000):

$$c(x, y, z, t) = \frac{C_0}{8} \left\{ \exp\left[\frac{(v-u')x'}{2D_x}\right] \operatorname{erfc}\left(\frac{x'-u't}{2\sqrt{D_x t}}\right) + \exp\left[\frac{(v+u')x'}{2D_x}\right] \operatorname{erfc}\left(\frac{x'+u't}{2\sqrt{D_x t}}\right) \right\} \left[ \operatorname{erfc} \frac{y-y_2}{2\sqrt{D_y\tau_m}} - \operatorname{erfc} \frac{y-y_1}{2\sqrt{D_y\tau_m}} \right] \left[ \operatorname{erfc} \frac{z-z_2}{2\sqrt{D_z\tau_m}} - \operatorname{erfc} \frac{z-z_1}{2\sqrt{D_z\tau_m}} \right] \quad (14)$$

191

192 where  $u' = \sqrt{v^2 + 4\lambda D_x}$ ,  $\tau_m = x/v$  and the first term of the product is the mono-dimensional  
 193 solution derived by Bear (1975).

194 If we have a plane source generating contamination with exponential decay, being  $\lambda_s$  the  
 195 decaying constant of the source, i.e.:

$$196 \quad r = r_0 f(t_0) = r_0 f(t - \tau) = r_0 \exp(-\lambda_s(t - \tau)) \quad (15)$$

197 eqn.(13) can be extended as:

$$198 \quad c(x, y, z, t) = \frac{C_0 x'}{8\sqrt{\pi D_x}} \int_0^t \exp(-\lambda_s(t - \tau)) \exp\left[-\lambda \tau - \frac{(x' - v\tau)^2}{4D_x \tau}\right] \left[ \operatorname{erfc} \frac{y - y_2}{2\sqrt{D_y \tau}} - \operatorname{erfc} \frac{y - y_1}{2\sqrt{D_y \tau}} \right] \left[ \operatorname{erfc} \frac{z - z_2}{2\sqrt{D_z \tau}} - \operatorname{erfc} \frac{z - z_1}{2\sqrt{D_z \tau}} \right] \frac{1}{(\tau)^{3/2}} d\tau \quad (16)$$

199 that is the solution in integral open form for a plane source with exponential decay as a boundary  
 200 condition of the first type. This solution is used in BIOSCREEN-AT (Karanovic et al., 2007).

201

### 202 **The proposed 3D solution for a plane source with exponential decay**

203 The closed form solution developed here is based on the "extended pulse approximation" that  
 204 uses spatial extensions of the well known instantaneous finite pulse models. This approximated  
 205 solution can be easily derived by following the approach proposed in Domenico and Robbins  
 206 (1985) and Martin-Hayden and Robbins (1997). Alternatively, the proposed solution can be  
 207 obtained from the instantaneous pulse solution, by following the three steps defined in rules (A),  
 208 (B) and (C) and by making some simplifying hypothesis.

209 The closed form approximate solution can be written as:

$$210 \quad c(x, y, z, t) = \frac{C_0}{8} \{g_x(t)\} \{g_y(t)\} \{g_z(t)\} \quad (17)$$

211 To construct the 3D solution of eqn.(1) subject to (9), (10), (11) and (12), where

212  $f(t) = \exp(-\lambda_s t)$ , i.e. valid for semi-finite domain in x, infinite domain in y and z, and subject

213 to a first type boundary condition described as a finite plane decaying source, we can use the  
214 following functions:

215 i) in eqn. (17) the term  $g_x$  is taken from the solution  $c(x, t) = \frac{c_0}{2} g_x$  of the 1D ADE (obtained by  
216 eliminating terms in  $y$  and  $z$  from eqn.(1)) subject to a first type boundary condition described  
217 as an exponential decaying source. This solution was given in the most general case by Van  
218 Genuchten and Alves (1982) and named C13, and it was later proposed by Williams and  
219 Tomasko (2008) for a particular case;

220 ii) the two terms  $g_y$  and  $g_z$  come from the solutions  $c(y, t) = \frac{c_0}{2} g_y$  and  $c(z, t) = \frac{c_0}{2} g_z$  of two  
221 independent 1D equations with dispersion, no advection and no reaction, valid for infinite  
222 domain and subject to instantaneous finite linear sources, defined respectively in  $y_1 \leq y \leq y_2$   
223 and in  $z_1 \leq z \leq z_2$ .

224 Since the proposed approximation combines the solution in  $x$  obtained for a continuous source  
225 with the solutions in  $y$  and  $z$  obtained for instantaneous sources to construct the final solution, a  
226 fixed time  $t$  has to be defined to calculate at each  $x$  the contribution of the instantaneous  
227 spreading terms in  $y$  and  $z$ . By following the Domenico and Robbins (1985) approximation,  $g_y$   
228 and  $g_z$  in eqn.(17) are computed at the apparent residence time  $\tau_m = x / v$  and the contribute of  
229 these two spreading terms in diluting concentration during time is calculated as at steady state.  
230 The physical meaning of this choice was explained by the plug flow model approximation in  
231 Domenico (1987).

232 The final solution is:

$$c(x, y, z, t) = \frac{C_0}{8} \left\{ \exp \left[ \frac{(v-u)x'}{2D_x} - \lambda_s t \right] \operatorname{erfc} \left( \frac{x'-ut}{2\sqrt{D_x t}} \right) + \exp \left[ \frac{(v+u)x'}{2D_x} - \lambda_s t \right] \operatorname{erfc} \left( \frac{x'+ut}{2\sqrt{D_x t}} \right) \right\} \\ \left[ \operatorname{erfc} \frac{y-y_2}{2\sqrt{D_y \tau_m}} - \operatorname{erfc} \frac{y-y_1}{2\sqrt{D_y \tau_m}} \right] \left[ \operatorname{erfc} \frac{z-z_2}{2\sqrt{D_z \tau_m}} - \operatorname{erfc} \frac{z-z_1}{2\sqrt{D_z \tau_m}} \right]$$

(18)

$$\text{with } u = \sqrt{v^2 + 4D_x \lambda - 4D_x \lambda_s}.$$

The alternative method to obtain eqn. (18) uses GFM and rules (A), (B) and (C) to derive the open integral form solution given by eqn. (16). Then the simplifying hypothesis consists in "reinterpreting time  $t$  as  $x/v$  for a moving coordinate system, as is common in all transverse spreading models" (Domenico and Robbins 1985). This translates in the substitution of time  $t$  in the transverse spreading terms of eqn. (16) with the apparent residence time  $\tau_m = x/v$ . With this substitution the two last terms of eqn. (16) do not depend on time, and the integration in time of eqn.(16) reduces to the integration in time of the 1D ADE, with first order reaction and subject to an exponential source decay as a first type boundary condition, that again leads to eqn.(17).

## Evaluation of Model Relative Errors

We want to compare eqn. (18), i.e. the approximated 3D analytical solution here proposed in closed-form for a plane source with exponential source decay, and eqn. (16), i.e. the 3D analytical solution in open form under the same conditions. We suggest an approach different from those adopted by Srinivasan et al. (2007) and West et al. (2007).

The main goal is to quantify relative errors in order to propose a short-cut method, based on simple diagrams, that allows the users of the closed form models to correct their results or to evaluate uncertainty of model output. Since the analytical solution here proposed in eqn. (18) and eqn. (16) are more general than the existing ones, the method is valid also for error analysis of

254 the analytical solutions contained in BIOSCREEN and BIOCHLOR. However, to show and  
 255 compare results of the method, we use the same values adopted in Srinivasan et al. (2007), even  
 256 if it could be observed that some chosen values are not consistent with some dispersivity  
 257 estimates.

Parameter	Value	
Longitudinal dispersivity ( $\alpha_x$ )	42.58	m
Transverse dispersivity ( $\alpha_y$ )	8.43	m
Transverse dispersivity ( $\alpha_z$ )	0.00642	m
velocity (v)	0.2151	m/d
Source width in Y direction (Y)	240.0	m
Source width in Z direction (Z)	5.0	m
Source concentration ( $C_0$ )	850	mg/l
Simulation time ( $t_m$ )	5110	d
First order reaction constant ( $\lambda$ )	0.001	s <sup>-1</sup>

258 **Table 1.** Simulation data

259 As shown in Gelhar et al. (1992) and Zheng and Bennett (2002), high-reliability  
 260 estimates of longitudinal dispersivities range from about 0.5 to 4 m and high-reliability estimates  
 261 of horizontal transverse dispersivities range from about 0.02 to 0.1 m. The values of  
 262 dispersivities here adopted to quantify relative errors are more than one order of magnitude  
 263 greater than the expected ones for real cases. Since Srinivasan et al. (2007) proved that the  
 264 approximated closed form solution of eqn. (14) relaxes to the Wexler (1992) analytical solution  
 265 for axial dispersivity tending to zero, the choice of a very high value of axial dispersivity is  
 266 conservative for this study, since the effects on relative errors will be increased with respect to  
 267 the real ones. Furthermore, since West et al. (2007) proved that for small transverse dispersivities  
 268 errors reduce in the centerline, simulations here proposed with a value of horizontal transverse

269 dispersivity almost two orders of magnitude greater than the expected one will produce higher  
 270 relative errors in the centerline than the expected real ones.

271 Dispersion coefficients used in this analysis are expressed by the product of dispersivities  
 272 and velocity.

273 Simulations are performed at different values of the exponential source decay constant  $\lambda_s$ ;  
 274 in this way also the comparison of the Domenico-modified closed-form solution given in  
 275 eqn.(14) with the Wexler (1992) analytical open form solution given in eqn. (13) are included.  
 276 Values of  $\lambda_s$  and  $\lambda$  are chosen in order to analyze all the known particular solutions included in  
 277 eqn. (16) and eqn. (18).

278 For certain uncommon values of  $\lambda_s$  the term under the square root defining  
 279  $u = \sqrt{v^2 + 4D_x\lambda - 4D_x\lambda_s}$ , also present in the well known one-dimensional solution proposed by  
 280 van Genuchten and Alves (1982), can be negative. In this case eqn. (18) must be computed by  
 281 using tools that treat complex exponential and complex error functions, such as Maple™  
 282 (trademark of Waterloo Maple Inc.), so that concentration is always a real number.

283 Simulation cases here reported are shown in table 2:

Parameters		Case	Corresponding simplified solutions
$\lambda$ [s <sup>-1</sup> ]	$\lambda_s$ [s <sup>-1</sup> ]		
0.0	0.0	a $u=u'=v$	conservative solute, no source decay.
0.001	0.0	b $u=u'>v$	eqns. (13) and (14).
0.001	0.0008	c $u>v$	



0.001	0.001	d
		$u=v$
0.001	0.0018	e
		$u < v$
0.001	0.0023	f
		$u=0$

**Table 2.** values of the decay constants and relative cases.

284

285

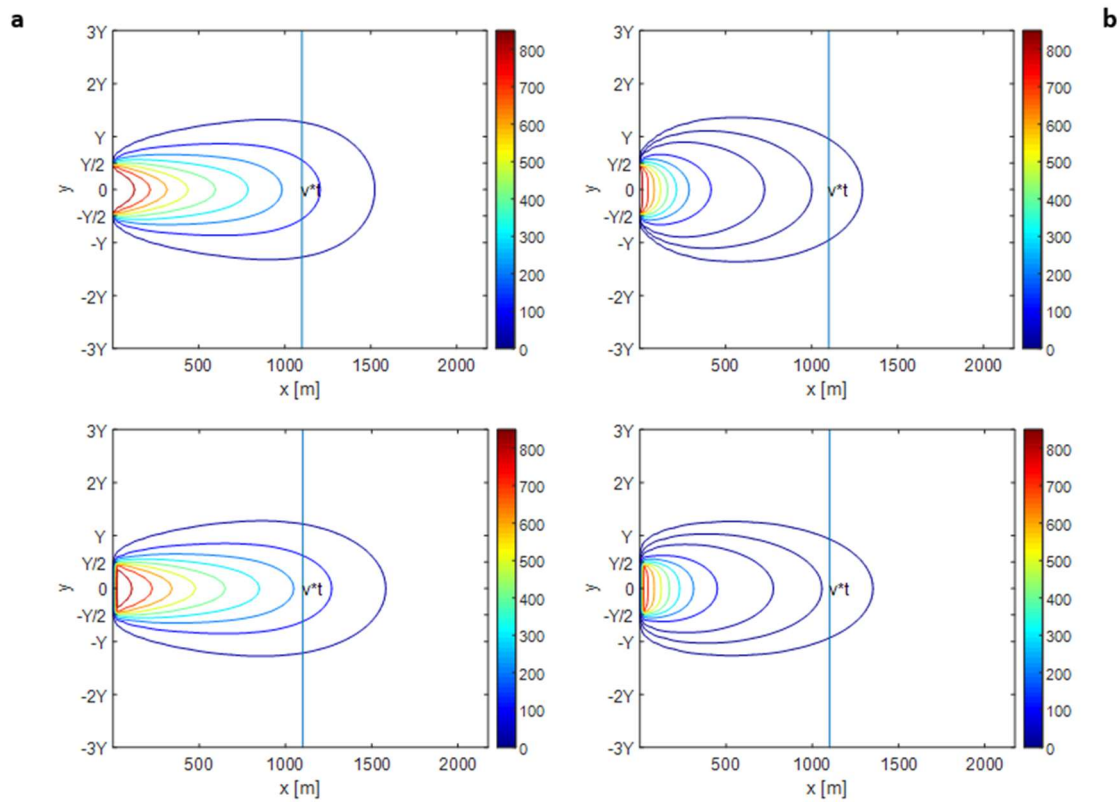
## 286 **Concentration field**

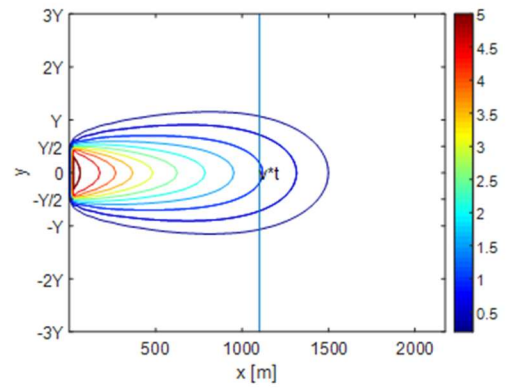
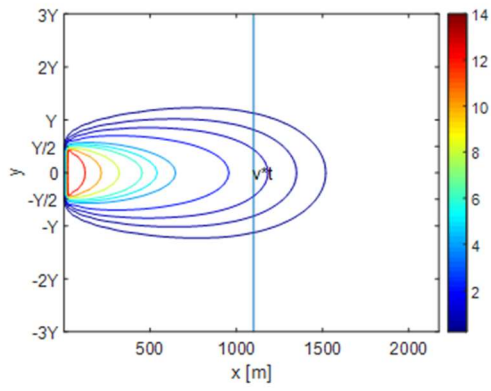
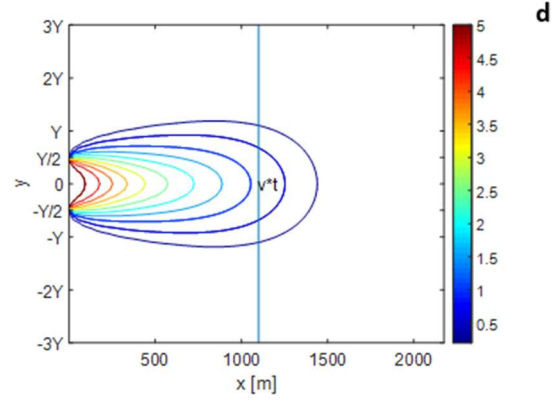
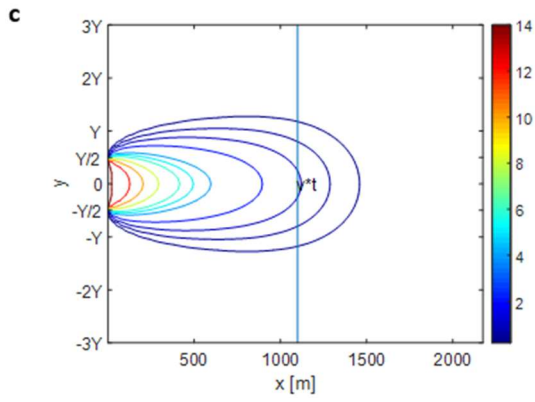
287 Some concentration fields evaluated by eqn. (18) and eqn. (16) at changing  $\lambda_s$  are plotted  
 288 in the (x,y) plane and reported in figure 1. Since in this study we considered the analytical 3D  
 289 solutions with infinite z domain, no differences between the contour shapes in y and z are to be  
 290 outlined, apart the obvious influence of the different source extensions and dispersion  
 291 coefficients. Hence concentration fields in (x,z) plane are essentially identical.

292 The numerical integration of eqn. (16) was made by adaptive Gauss-Kronrod quadrature  
 293 method (available in QUADPACK library, GNU Scientific Library, Matlab QUADGK, NAG  
 294 Numerical Libraries and R). For each subplot of figure 1 the upper concentration contour map  
 295 was developed using the approximate closed form proposed in eqn. (18) and the lower one is  
 296 evaluated by the exact open integral form expressed by eqn. (16). The vertical line is the  
 297 advective front, i.e. the distance  $\underline{x}$  from the source where a conservative contaminant injected  
 298 with a Dirac function would be found without dispersion effects at  $t=t_m$ .

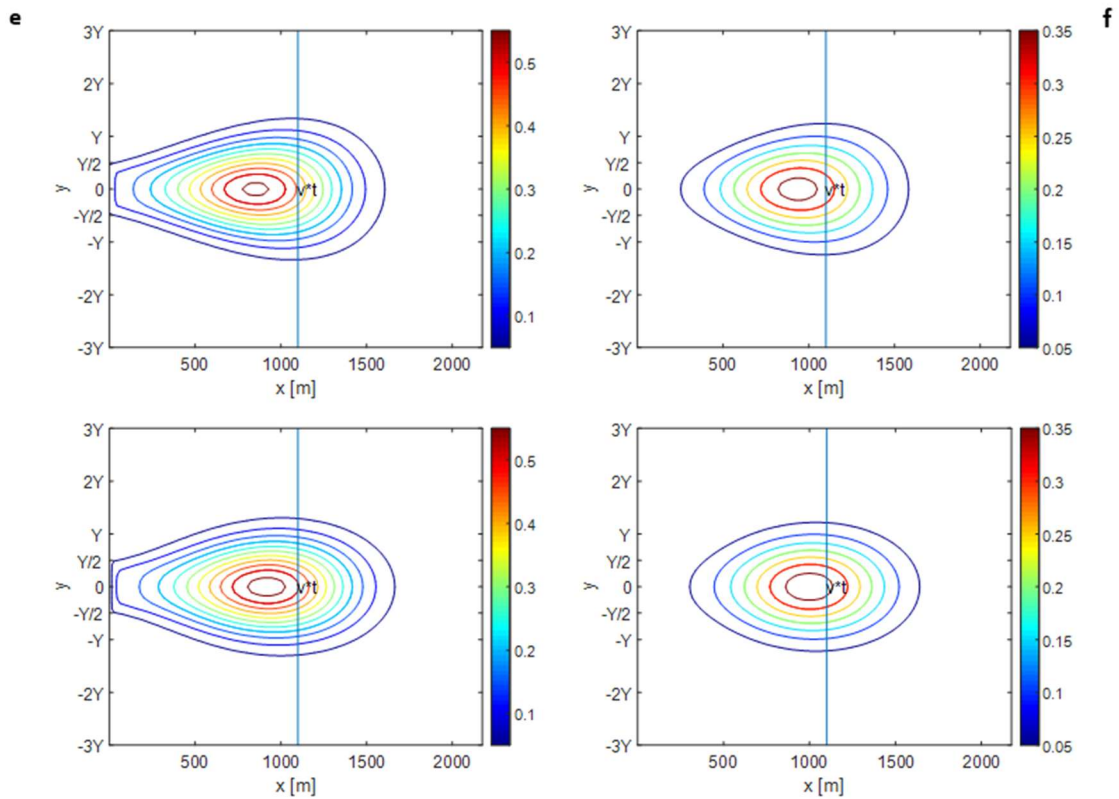
299 Case a) represents model outputs in the simple situation of advection-dispersion of a  
 300 conservative solute released at constant concentration by a plane source. Case b) compares  
 301 models outputs for a non-conservative solute underlying a first order decay and released at

302 constant concentration by a plane source. Finally, cases c), d), e), f) represent concentration  
303 contours for a non-conservative solute subject to first order decay, released by decaying plane  
304 sources with varying decay constants and effective velocities.





□



305 **Figure 1.** Concentration maps. Approximated closed form (top) versus integral open form  
 306 (bottom). Case a) conservative solute, no source decay. Case b) reacting solute, no source decay.  
 307 Cases c) to f) reacting solute, source decay.

308

309 It can be observed that concentration distributions evaluated by eqn. (18), are more  
 310 delayed with respect to the advective front than distributions obtained by eqn. (16). The graphs  
 311 show that the delay increases with  $\lambda_s$ . By observing cases e) and f) at simulation time  $t_m=5110$   
 312 [s], when the source is already consumed, the centre of the plume, i.e. the point at maximum  
 313 concentration, evaluated with the closed form solution, lags behind with respect to the  
 314 concentration profiles computed by eqn. (16).

315 The initial value of concentration is set at  $C_0=850\text{mg/l}$ ; case a) is the one with the higher  
316 concentration in the domain since a conservative contaminant is considered. By comparing the  
317 well known case a) and case b) at equal distance from the source, graphs confirm the effect of  
318 first order decay in reducing contaminant concentration in the domain. The effect of the first  
319 order reaction in mean contracting the shape of the iso-concentration curves can be also noticed.  
320 This effect can be directly correlated to the value of the effective velocity  $u'$  appearing in eqn.  
321 (14), where  $u'$  is higher than  $v$ .

322 By looking at cases c) and d) it's interesting to observe how the shape of concentration  
323 contours in the domain stretches again under the reduction of the effective velocity  $u$  appearing  
324 in eqn. (18). This decrease is due to the term containing the zero order source decay, that has  
325 opposite sign with respect to the first order reaction term, both contained in the expression of the  
326 effective velocity appearing in eqn. (18). Consequently, for case d), in which  $\lambda=\lambda_s$ , giving  $u=v$ ,  
327 the shape of the iso-concentration distributions are identical to case a).

328 Finally, in cases e) and f) for which  $u$  is less than  $v$ , the shape of concentration contours  
329 changes again allowing to observe the effect of source diminishment.

330

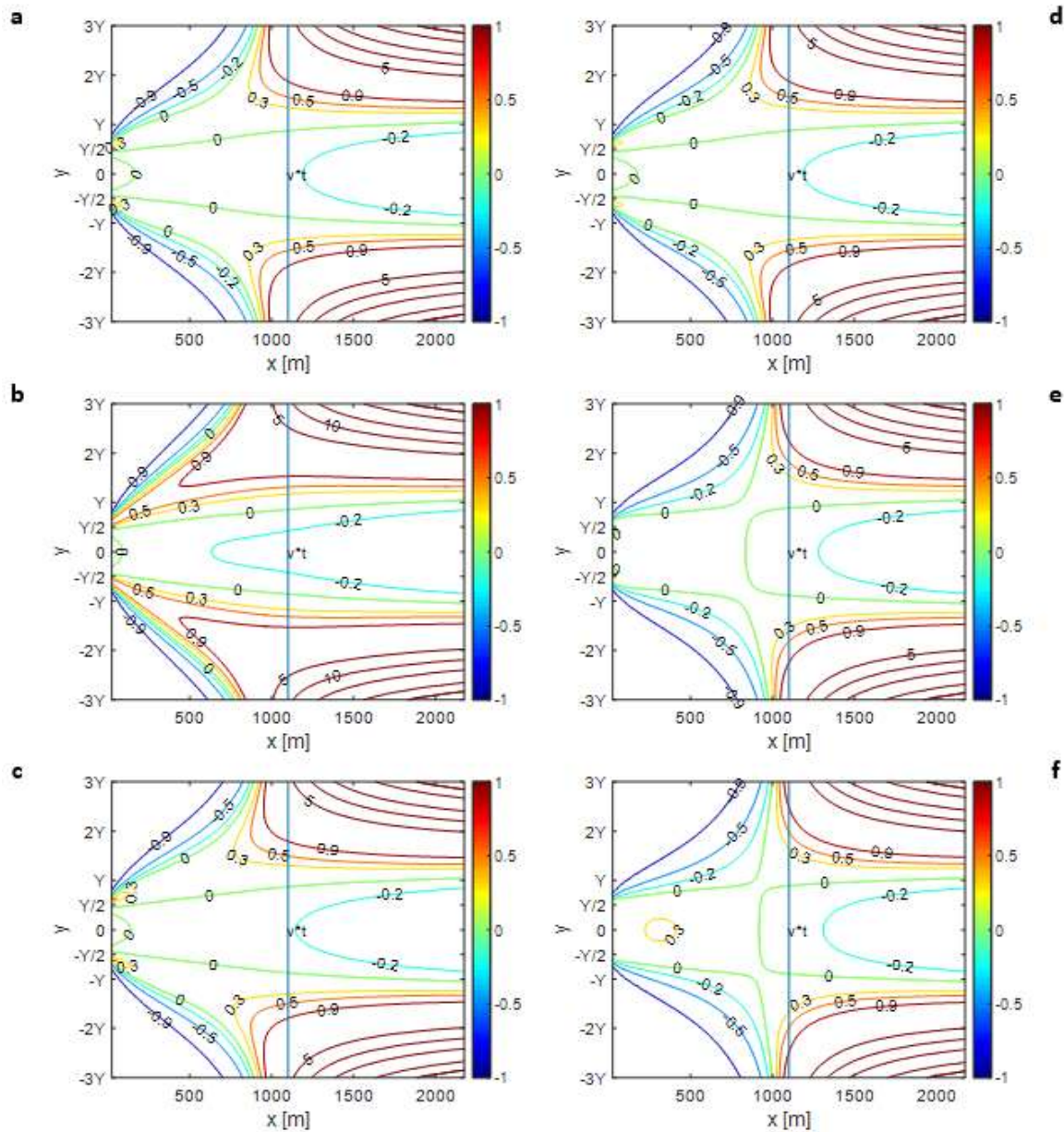
### 331 **Relative differences**

332 Relative differences between the closed form solution and the integral one, expressed as:

$$333 \quad E_r = \frac{C - I}{I} \quad (18)$$

334 are shown in the ray-shaped diagrams of figure 2. The symbol  $C$  indicates the closed form  
335 solution with the same type of approximation adopted by Martin-Hayden and Robbins (1997),  
336 also called Domenico modified; and the symbol  $I$  the integral open form solution. Diagrams in

337 figure 2 are plotted at fixed simulation time  $t=5110$  days and at changing  $\lambda_s$ . The vertical line in  
 338 the figure is the advective front, as previously defined. The reported cases are the same as  
 339 illustrated in figure 1.



340  
 341 **Figure 2.** Diagrams of relative errors at fixed simulation time. Case a) conservative solute, no  
 342 source decay. Case b) reacting solute, no source decay. Cases c) to f) reacting solute, source  
 343 decay.

344

345           Three error zones can be distinguished in figure 2. The first one lies along the centerline  
346 and extends in the  $y$  direction for a width slightly greater than the source width  $Y$ . The other two  
347 zones are separated by the vertical line describing the advective front and posed at  $\underline{x} = v \cdot t_m$ . This  
348 vertical line is an asymptote for the relative errors contours at  $y$  tending to  $\pm$ infinity. The  
349 existence of this asymptote is due to the fact that both the solutions satisfy the boundary  
350 condition at  $y$  tending to infinity. In the zone on the left of the asymptote, the closed form  
351 approximated solution underestimates the concentration, however in the zone on the right of the  
352 asymptote the approximated solution overestimates the concentration. It is very important to  
353 notice that in these two zones concentration values are more than three orders of magnitude  
354 lower than the source concentration.

355           Along the centerline in figure 2, the relative error is always negative for cases a) to d),  
356 where the effective velocity  $u$  is greater (or equal) than the pore space velocity  $v$ . For these four  
357 cases the approximate closed form solution underestimates concentrations on the centerline and  
358 also in the domain space of width  $Y$  along the centerline. However, the maximum  
359 underestimation is only 10% for concentration values up to two orders of magnitude lower than  
360 the source concentration value. Cases e) and f), when  $u$  is less than the pore space velocity  $v$ ,  
361 show a particular behaviour behind the advective front: the relative error is positive and the  
362 approximated closed form solution can overestimate concentration values. Looking at the lateral  
363 zone behind the advective front and on the left of the asymptote, negative relative errors have to  
364 be weighted in comparison to concentration values. For all the six cases a) to f) the  
365 underestimation of the transverse dispersion effects on concentration produced by eqn. (18) gives

366 relative errors, which, when greater than 20%, are related to values of concentration less than  
367 two orders of magnitude of the initial concentration of the source.

368 Finally, as regards the lateral zone beyond the advective front and on the right of the  
369 asymptote where the closed form solution overestimates concentration levels, very high relative  
370 errors are related to concentration values that are more than four orders of magnitude less than  
371 the initial concentration, hence these errors are insignificant. As regards cases c) to f) subject to  
372 the decaying source, it has to be noted that concentration values are not very high also on the  
373 centerline, so the relative errors observed in the two zones are related to concentration values that  
374 are very small. As an example, in case f) the centre of the plume, i.e. the point at maximum  
375 concentration, has a concentration value of about 0.45mg/l.

376 It is interesting to outline that ray diagrams of case a) and case d) are identical, so the  
377 effective velocity  $u$  can be used as a parameter influencing relative error diagrams.

378 With reference to table 1, a complete analysis of relative errors should take into  
379 consideration six chemical-physical parameters, i.e. the three dispersivities, space velocity and  
380 the two decay constants; three parameters derived from initial and boundary conditions, i.e.  
381 source widths  $Y$  and  $Z$  and initial concentration  $C_0$ ; simulation time  $t_m$ .

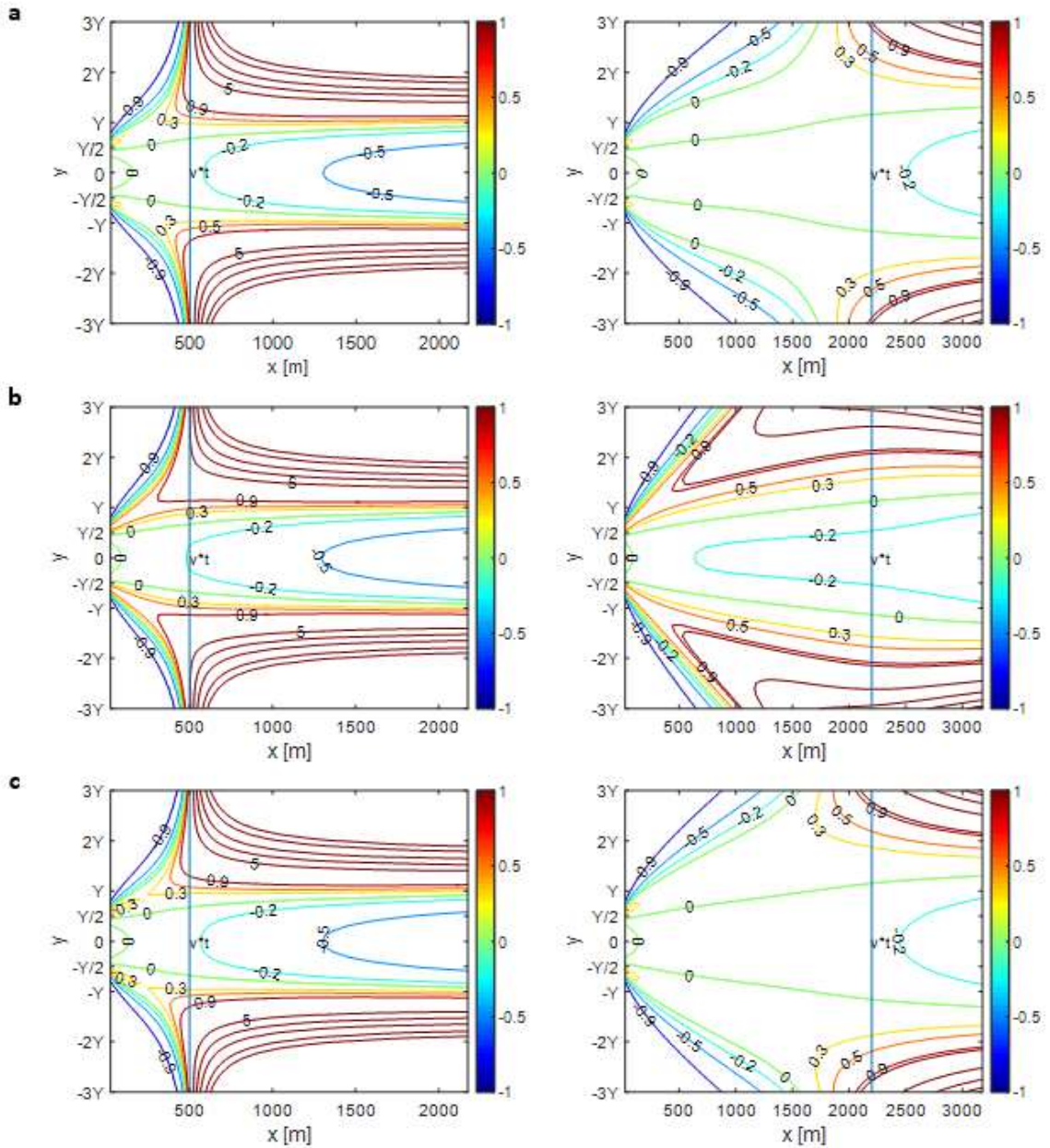
382 Since simulation time  $t_m$  is not correlated with dimensionless numbers but it is very  
383 important for the validity of the Domenico and Robbins approximation, we report here its effects  
384 at different  $\lambda_s$  values.

385



386 Time dependence

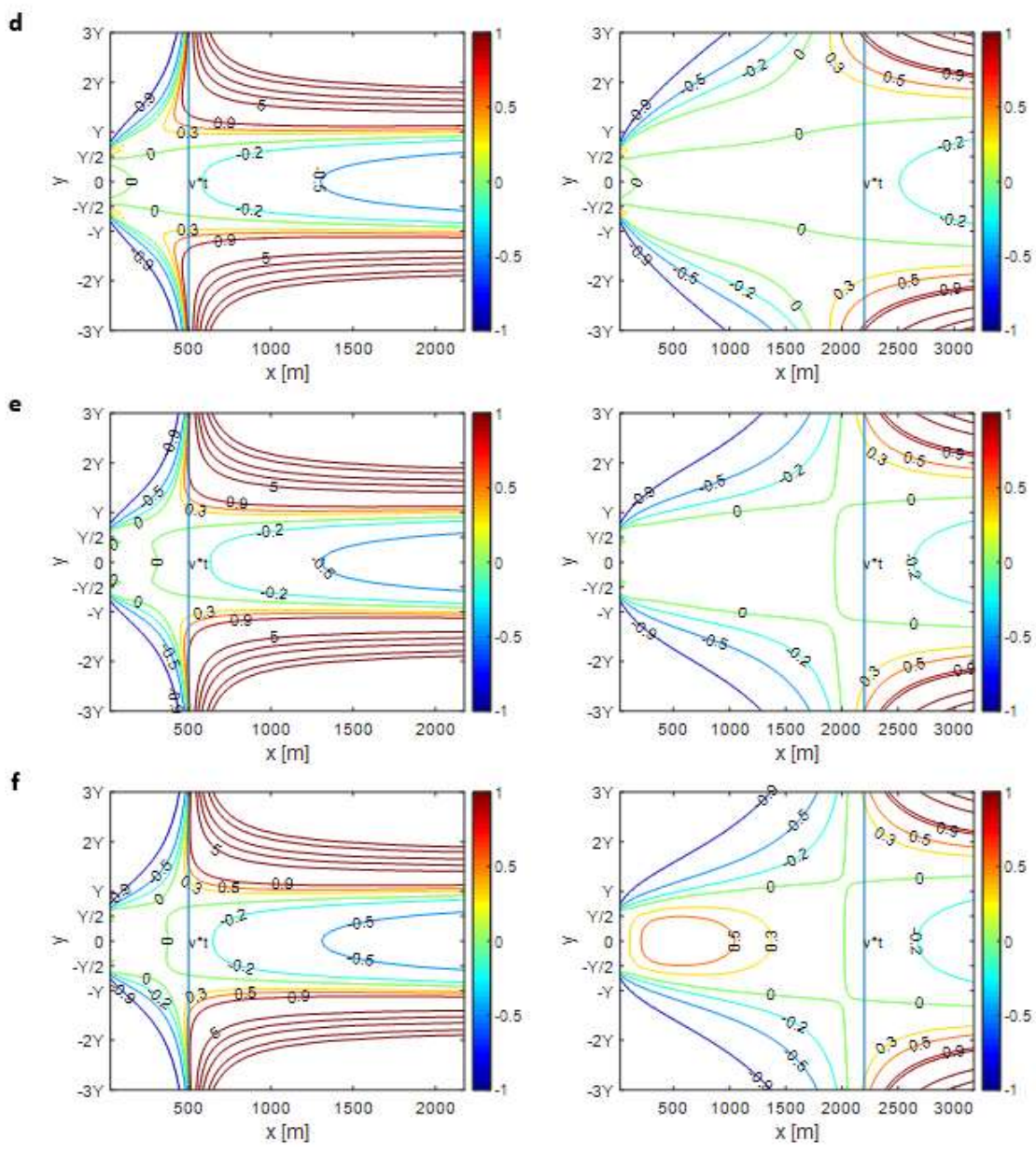
387 Some simulations have been carried out in order to observe how the diagrams vary at  
388 changing  $t_m$ . In figure 3 and figure 4 ray-diagram modifications at  $t_m/2$  and  $2t_m$  are shown.



389

390 **Figure 3.** Diagrams of relative errors at half simulation time (left) and double simulation time  
 391 (right). Case a) conservative solute, no source decay. Case b) reacting solute, no source decay.  
 392 Case c) reacting solute, source decay.

393



394

395 **Figure 4.** Diagrams of relative errors at half simulation time (left) and double simulation time  
396 (right). Cases d) to f) reacting solute, source decay.

397

398 In the zone of width  $Y$  along the centerline, at half simulation time  $t = t_m/2$ , small relative  
399 errors behind the advective front can be observed. On the contrary, negative relative errors are  
400 observed far from the centerline and on the left hand side of the asymptote are present.  
401 Overestimation errors are observed far from the centerline and on the right hand side of the  
402 asymptote. If the amplitude of relative errors is again evaluated with reference to the ratio  
403 between the actual concentration and the initial one, it is easy to observe that the supposed higher  
404 relative errors, for example in figure 3 case c) at  $x=600$ ,  $y=-2Y$  where  $Er=5$ , are related to lower  
405 concentration values as  $c=2*10^{-4}$  mg/l).

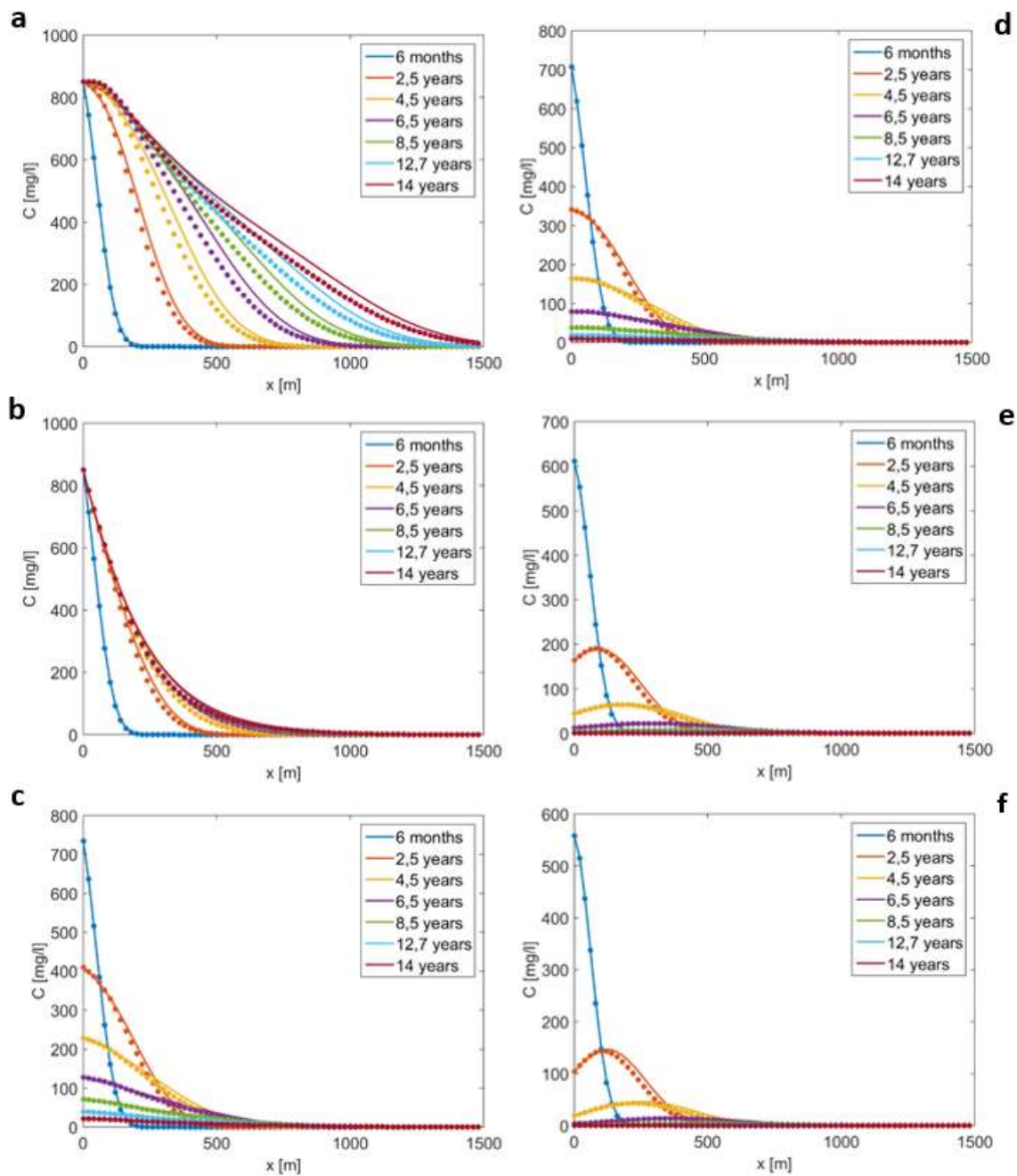
406 Ray diagrams of case a), i.e. conservative solute, and case d) in which  $u=v$ , are identical.  
407 For double simulation time, it's important to notice how the approximate solution overestimates  
408 concentration in the zone along the centerline and behind the advective front and underestimates  
409 beyond the advective front in cases e) and f), i.e. when  $u$  is less than  $v$  and the plume detaches  
410 from the boundary. Again cases a) and d) have the same relative error.

411

#### 412 **Centerline profiles near source**

413 In order to better analyze the results of the proposed solution for small simulation times  
414 and near the source of contamination, some concentration profiles in the centerline are presented  
415 in figure 5 for cases of table 2 at changing simulation times.

416 Concentration profiles at different values of  $\lambda_s$  are plotted as a continuous line for the  
 417 exact integral solution and as a dotted line for the approximated closed form solution.



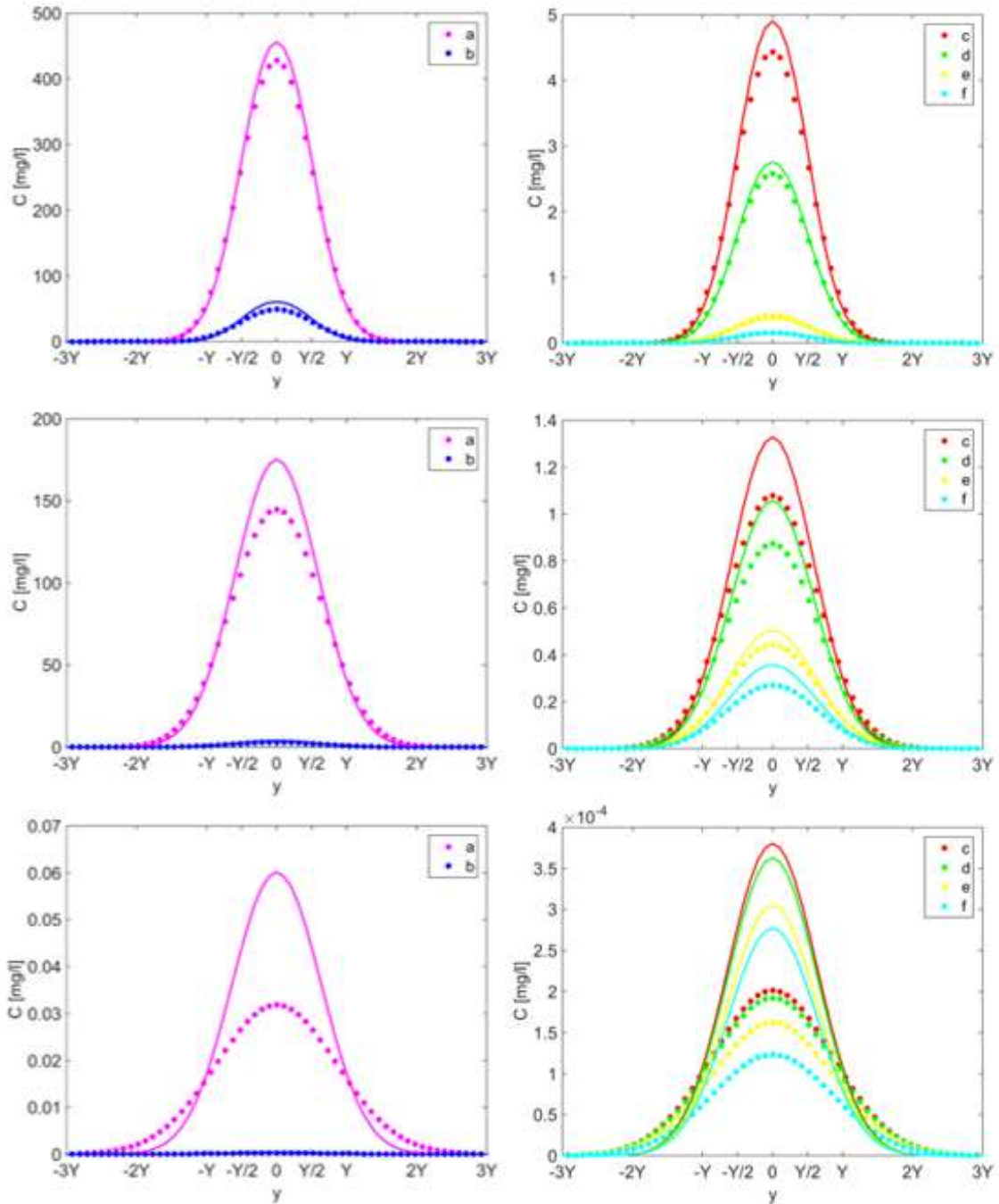
418  
 419 **Figure 5.** Concentration profiles in the centerline at changing simulation time. Approximated  
 420 closed form (dotted) versus integral form (continuous). Case a) conservative solute, no source  
 421 decay. Case b) reacting solute, no source decay. Cases c) to f) reacting solute, source decay.

422

423 **Transverse profiles**

424 Transverse profiles were analyzed with respect to the advective front, i.e. the distance  $\underline{x}$   
425 from the source where a conservative contaminant injected with a Dirac function would be found  
426 without dispersion effects at  $t=t_m$ . In figure 6 three transverse sections at  $x=x/2$ ,  $x=x=v*t_m$  and  
427  $x=2x$  are plotted, where concentration profiles at different values of  $\lambda_s$  are represented as a  
428 continuous line for the exact integral solution and as a dotted line for the approximate closed  
429 form solution.





430

431 **Figure 6.** Concentration profiles in three transverse sections at  $x=\underline{x}/2$  (top),  $x=\underline{x}=v*t_m$  (center)

432 and  $x=2\underline{x}$  (bottom) for the approximated closed form (dotted) and the integral form

433 (continuous). Case a) conservative solute, no source decay. Case b) reacting solute, no source

434 decay. Cases c) to f) reacting solute, source decay.

435

436 Cases a) and b) are plotted on the left hand side of figure 6 and cases c) to f) on the right  
437 hand side. Cases c) to f) are plotted in different graphs since concentration values are much  
438 smaller than in cases a) and b), due to source consumption in time.

439 In the region of space far from the centerline the closed form solution overestimates  
440 concentration values. This effect increases with values of  $\lambda_s$  but at lower concentration values.

441 By observing figure 6 for all cases a) to f) the value of  $y$  where the two solutions  
442 converge can be determined. It lies in the intervals  $(-2Y, -Y/2)$  and  $(Y/2, 2Y)$ .

443

## 444 **Conclusions**

445 A three-dimensional approximate closed form solution with source decay has been  
446 presented and compared with the exact solution contained in BIOCHLOR-AT. Relative error  
447 diagrams are presented that define areas in the flow field where use of the closed form solution  
448 results in minimum error. The study focused on the errors associated with source decay and the  
449 effect of simulation time. The concentration profiles given in the form of contours, longitudinal  
450 sections and transverse sections, confirm that the closed form solution can be used with  
451 acceptable errors in the entire central area of a width at least equal to the source width, both  
452 behind and beyond the advective front and with underestimation maximum errors of 20-25% for  
453 concentration values up to two orders of magnitude less than the initial source concentration. In  
454 the case of source decay, at high simulation times an overestimation error sometimes appears  
455 near the source of up to 50% but in these cases concentration values are about three orders of  
456 magnitude lower than the initial source concentration. It is finally confirmed that the closed and

457 the open form models give different results far from the centerline beyond the advective front,  
458 but this situation corresponds again to negligible values of concentration.

459

## 460 **Acknowledgments**

461 The authors wish to thank the anonymous Associate Editor and reviewers, and the Executive  
462 Editor Dr. Schincariol for their constructive comments and suggestions. The paper constitutes  
463 cooperative research between the Università degli Studi di Genova and the University of  
464 Connecticut. The authors wish to commemorate the late Dr. Patrick Domenico for his  
465 contributions to risk assessment modeling that inspired this research and that of many others.

466

## 467 **References**

468

- 469 Aziz, C.E., C.J. Newell, J.R. Gonzales, P. Haas, T.P. Clement, and Y. Sun. 2000. BIOCHLOR—  
470 Natural attenuation decision support system, User's Manual v. 1.0., U.S. Environmental  
471 Protection Agency Report EPA/600/R-00/008. EPA Center for Subsurface Modeling  
472 Support (CSMOS), Ada, Oklahoma.
- 473 Baetsle, L.H. 1969. Migration of Radionuclides in Porous Media. In: A. M. F. Duhamel (Ed.),  
474 Progress in Nuclear Energy Series XII, Health Physics, 707-730.
- 475 Batu, V. 1989. A generalized two-dimensional analytical solution for hydrodynamic dispersion  
476 in bounded media with the first-type boundary conditions at the source, Water Resource.  
477 Research, 25, 1125-1132.



478 Batu, V. 1993. A generalized two-dimensional analytical solute transport model in bounded  
479 media for flux-type finite multiple sources, *Water Resource Research*, 29, 2881-2892.

480 Batu, V. 1996. A generalized three-dimensional analytical solute transport model for multiple  
481 rectangular first-type sources, *Journal of Hydrology*, 174, 57-82.

482 Bear, J. 1972. *Dynamics of fluids in Porous Media*. Elsevier, New York, USA.

483 Bosma, W.P., and S.E.A.T.M. Van der Zee. 1993. Transport of reacting solute in a one-  
484 dimensional, chemically heterogeneous porous medium, *Water Resource Research*, 29,  
485 117-131.

486 Domenico, P.A. 1987. An analytical model for multidimensional transport of a decaying  
487 contaminant species, *Journal of Hydrology*, 91, 49-58.

488 Domenico, P.A., and G.A. Robbins. 1984. A new method of contaminant plume analysis,  
489 *Ground Water*, 23, 476-485.

490 Ford, R. G., R.T. Wilkin, and R. W. Puls (eds). 2007. *Monitored Natural Attenuation of*  
491 *Inorganic Contaminants in Ground Water, Vol. 1 - Technical Basis for Assessment.*  
492 EPA/600/R-07/139, U.S. Environmental Protection Agency, Office of Research and  
493 Development, National Risk Management Research Laboratory, Ada, Oklahoma.

494 Gelhar, L.W., C. Welty and K. R. Rehfeldt. 1992. A critical review of data on field-scale  
495 dispersion in aquifers, *Water Resource Research*, 28, 7, 1955–1974.

496 Greenberg, M.D., 1971. *Application of Green's Functions in Science and Engineering*. Prentice-  
497 Hall, Englewood Cliffs, NJ.

498 Guyonnet, D., and C. Neville. 2004. Dimensionless analysis of two analytical solutions for 3-D  
499 solute transport in groundwater, *Journal of Contaminant Hydrology*, 75(1–2) 141–153.

500 Hongtao, W., L. Jinwen, Z. Yan, L. Wenjing, and W. Huayong. 2011. Stepwise superposition  
501 approach for the analytical solutions of multi-dimensional contaminant transport in finite-  
502 and semi-finite aquifers, *Journal of Contaminant Hydrology*, 125, 86-101.

503 Karanovic M., C.J. Neville, and C.B. Andrews. 2007. BIOSCREEN-AT: BIOSCREEN with an  
504 Exact Analytical Solution, *Ground Water* 45, 242-245.

505 Leij, F.J., N. Toride, and M.Th. van Genuchten. 1993. Analytical solutions for non-equilibrium  
506 solute transport in three-dimensional porous media, *Journal of Contaminant Hydrology*,  
507 151, 193-228.

508 Leij, F.J., E. Priesack, and M.G. Schaap. 2000. Solute transport modelled with Green's functions  
509 with application to persistent solute sources, *Journal of Contaminant Hydrology*, 41, 155-  
510 173.

511 Leij, F.J., T.H. Skaggs and M.Th. van Genuchten. 1991. Analytical solution for solute transport  
512 in three-dimensional semi-infinite porous media, *Water Resource Research*, 27(10),  
513 2719-2733.

514 Martyn-Hayden, J., and G.A. Robbins.1997. Plume distortion and apparent attenuation due to  
515 concentration averaging in monitoring wells, *Ground Water*, 35 (2), 339–346.

516 Neville, C. J. 1994. *Compilation of Analytical Solutions for Solute Transport in Uniform Flow*,  
517 S.S. Bethesda, MD, USA: Papadopus & Associates.

518 Newell, C., R. McLeod and J. Gonzales. 1996. BIOSCREEN, Natural Attenuation Decision  
519 Support System, User's Manual v.1.3., U.S. Environmental Protection Agency Report  
520 EPA/600/R-96-087. EPA Center for Subsurface Modeling Support (CSMOS), Ada,  
521 Oklahoma. (<http://www.epa.gov/ada/csmos/models/bioscrn.html>).

522 Park, E., and H. Zhan. 2001. Analytical solutions of contaminant transport from finite one-, two-,  
523 and three-dimensional sources in a finite-thickness aquifer, *Journal of Contaminant*  
524 *Hydrology*, 53, 41-61.

525 Roach, G.F., 1982. *Green's Functions*. Cambridge Univ. Press.

526 Sagar, B. 1982. Dispersion in three dimensions: Approximate analytic solutions, *ASCE Journal*  
527 *of the Hydraulics. Division*, 108(HY1), 47-62.

528 Srinivasan, V., T.P. Clement, and K.K. Lee. 2007. Domenico Solution—Is It Valid?, *Ground*  
529 *Water*, 45(2) 136–146. Van Genuchten, M. Th., and W.J. Alves. 1982. Analytical  
530 solutions to the one-dimensional convective –dispersive solute transport equation, U.S.  
531 Department of Agriculture Technical Bulletin No. 1661, USDA, Riverside, Calif.

532 Van der Zee, S.E.A.T.M. 1990. Analysis of soluted redistribution in heterogeneous field, *Water*  
533 *Resource Research*, 26, 273-278.

534 Wang, H., and H. Wu. 2009. Analytical solutions of three-dimensional contaminant transport in  
535 uniform flow field in porous media: A library, *Front. Environ. Sci. Engin. China*, 3(1),  
536 122-128.

537 West, M. R., B.H. Kueper, and M.J. Unga. 2007. On the Use and Error of Approximation in the  
538 Domenico (1987) Solution, *Ground Water*, 45(2), 126-135.

539 Wexler, E.J. 1992. Analytical solutions for one-, two-, and three-dimensional solute transport in  
540 ground-water systems with uniform flow, U.S. Geological Survey, *Techniques of water –*  
541 *Resources Investigations*, Book 3, Chap. B7.

542 Williams, G. P. and D. Tomasko. 2008. Analytical Solution to the Advective-Dispersive  
543 Equation with a Decaying Source and Contaminant, *Journal of Hydrologic Engineering*,  
544 13(12), 1193-1196.

545 Yeh, G.T., and Y.J. Tsai. 1976. Analytical three dimensional transient modelling of effluent  
546 discharges, *Water Resource. Research.*, 12, 533-540.

547 Yeh, G.T. 1981. Analytical transient one-,two-, and three-dimensional simulation of waste  
548 transport in the aquifer system, Oak Ridge National Laboratory, Report. ORNL-5602,  
549 Oak Ridge, Tennessee, USA.

550 Zheng, C., and G. D. Bennett. 2002. *Applied Contaminant Transport Modeling*, Wiley, ISBN:  
551 978-0-471-38477-9.

552